

Performance and operational aspects of LHCb's VELO and ST

Eduardo Rodrigues^{*†}

University of Manchester

E-mail: eduardo.rodrigues@cern.ch

The LHCb experiment aims at the search for New Physics with the study of rare heavy hadron decays and the study of CP violation in the decays of charm and beauty hadrons. The detector, a single-arm spectrometer at the Large Hadron Collider (LHC), Geneva, includes a high precision tracking system: a silicon-strip vertex detector, a silicon-strip tracker upstream of the magnet, and three stations of silicon-strip detectors and straw tubes downstream of the magnet. Results are presented for the performance of the silicon-strip detectors during the first LHC run, with emphasis on the most recent studies. Highlights will include alignment, cluster finding efficiency, single hit resolution, and impact parameter and vertex resolutions, with updates based on recent results from the 2012 LHC running.

*22nd International Workshop on Vertex Detectors,
15-20 September 2013
Lake Starnberg, Germany*

^{*}Speaker.

[†]On behalf of the LHCb VELO and ST groups.

1. Introduction

LHCb is the experiment [1] at the Large Hadron Collider (LHC) at the CERN laboratory, Geneva, dedicated to the study of heavy flavour particles. Its primary goals are indirect searches for New Physics (NP) in the decays of heavy hadrons and the study of CP violation and rare decays of heavy hadrons and leptons. The detector covers the pseudorapidity range from 2 to 5, as b -quark pairs are predominantly produced close to the beam line. The design of the LHCb detector considered the following system requirements crucial to its physics programme: (1) excellent separation between the interaction point – the primary vertex (PV) – and the secondary vertex from a heavy particle decay; (2) efficient tracking providing good momentum and impact parameter resolution for charged particles; (3) excellent decay time resolution capable of resolving the fast oscillations of the B_s^0 meson; and (4) a high-performance particle identification system to separate kaons and protons from pions in a wide momentum range. The tracking system, discussed in this paper, is central to all but the last of these requirements.

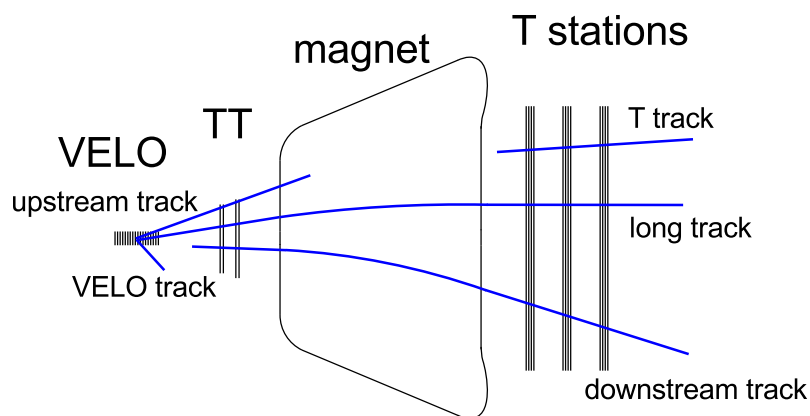


Figure 1: Schematic drawing of the LHCb tracking system. Also indicated are the track types reconstructed by the track finding algorithms at LHCb.

2. The LHCb tracking system

The LHCb tracking system – see the schematic drawing in Fig. 1 – comprises the vertex locator (VELO), the Tracker Turicensis (TT), the Inner Tracker (IT), a straw-tube Outer Tracker (OT) [2], and a dipole magnet with a bending power of 4 Tm in-between the upstream TT and the downstream IT and OT. IT and OT make, respectively, the inner and outer part of the downstream tracker. Solely the VELO, TT and IT are presented and discussed here, all of which are based on silicon micro-strip technology. Details of the LHCb detector are found elsewhere [1].

Vertexing at LHCb relies on the VELO, a silicon micro-strip detector surrounding the proton-proton interaction region. The VELO consists of two movable detector halves with 21 stations in total. Each detector module pairs two types of sensors to measure radial (R) and azimuthal angle (Φ) coordinates.

The modules are built from n-on-n $300\ \mu\text{m}$ thick half-disc sensors mounted on a carbon fibre support. The VELO is also equipped with the only n-on-p sensors operating at the LHC. Each sensor has 2048 strips, with the strip pitch increasing with radial distance from the beam-line; the pitch ranges from roughly $40\ \mu\text{m}$ at the inner edge to roughly $120\ \mu\text{m}$ in the outer regions.

Both detector halves are operated in a secondary vacuum, separated from the primary vacuum of the LHC beam by a $300\ \mu\text{m}$ thick Aluminium foil; the foil also insulates the VELO sensors from the radio frequency pick-up of the proton beams. The system is cooled with a bi-phase CO_2 cooling system at -28°C , maintaining the sensors at -7°C .

During running conditions, the active silicon strips get as close as $8.2\ \text{mm}$ from the colliding beams. However, during the beam set-up of the LHC, *i.e.* whenever the beams are not declared stable, both retractable detector halves are maintained in an open position at a distance of $3\ \text{cm}$ from the beams.

The two trackers downstream of the VELO are jointly referred to as the Silicon Tracker (ST); their total sensitive area of silicon amounts to approximately $12\ \text{m}^2$. TT is designed to cover the full acceptance in front of the magnet whereas IT, downstream of the magnet, covers the region around the beam with the highest particle fluence. Both TT and IT are p^+ -on-n micro-strip detectors, with the sensors being kept at 8°C .

The four detector planes of TT are arranged with a tilt following $(0^\circ, +5^\circ, -5^\circ, 0^\circ)$ with respect to the vertical axis. The $500\ \mu\text{m}$ thick sensors with a pitch of $183\ \mu\text{m}$ are bonded together to make read-out sectors between one and four sensors – depending on their area receiving more or less fluence. The maximum length of the four bonded sections is $37\ \text{cm}$.

IT is the ensemble of three stations, each of which is made of four boxes covering in total $120\ \text{cm}$ by $40\ \text{cm}$ in the plane transverse to the beams. The four planes of each station are arranged with the same tilt layout as TT, *i.e.* follow $(0^\circ, +5^\circ, -5^\circ, 0^\circ)$. Two sensor thicknesses are utilised: $320\ \mu\text{m}$ thick sensors for the boxes above and below the beam-pipe, and $410\ \mu\text{m}$ thick sensors for the boxes left and right of the vertical plane crossing the beam-line. The strip pitch is $198\ \mu\text{m}$ for both sensor thicknesses.

3. LHCb run I

The first run of the LHC, the so-called Run I, spanned the period 2010-12. In the years 2010 till 2011 both proton beams were brought to collision at a centre-of-mass energy of $7\ \text{TeV}$, while the energy increased to $8\ \text{TeV}$ for the 2012 running period. For the bulk of Run I the instantaneous luminosity was in the range $\mathcal{L} = 2 - 4 \times 10^{32}\ \text{cm}^{-2}\ \text{s}^{-1}$, with a total recorded luminosity of $3.2\ \text{fb}^{-1}$ (approximately 1.1 and $2.1\ \text{fb}^{-1}$ in 2011 and 2012, respectively). These conditions translated into an average number of interactions per bunch crossing in the range $\mu = 1.4 - 1.7$. These numbers are to be compared with the design running conditions of collisions at a centre-of-mass energy of $14\ \text{TeV}$: $\mathcal{L} = 2 \times 10^{32}\ \text{cm}^{-2}\ \text{s}^{-1}$ and $\mu = 0.4$. LHCb is particular in that a luminosity levelling was implemented to maintain a constant (instantaneous) luminosity during a fill. This was achieved by continuously steering the beams.

LHCb operated smoothly and very successfully over Run I, showing an average data taking efficiency around 90% in 2011 and 93% in 2012. The excellent performance of the accelerator can be inferred, for example, from the number of days in 2012 when the LHC provided pp -collision

data – approximately 200. Stable beams were in fact declared for 36% of the time, *i.e.* during approximately 76 days (x 24 hours).

4. Detector operation

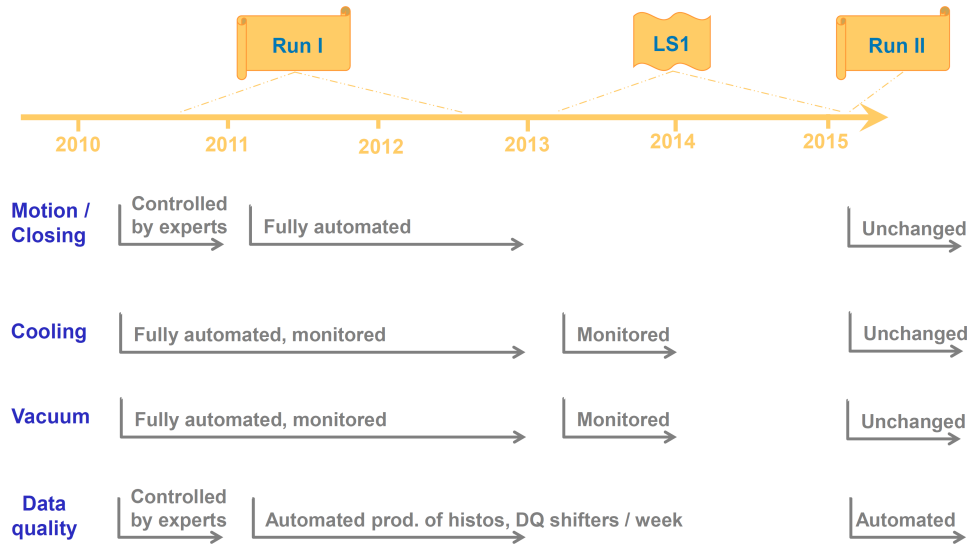


Figure 2: Schematic timeline summarising the operations of the VELO.

The operation of the VELO comprises four main aspects: the motion system for the closing of the two detector halves, for the collection of physics-quality data; the operation of the cooling system; that of the vacuum system; and the assessment of the quality of the data aimed at physics analysis. A schematic overview of the way the operation of the VELO was done during Run I is displayed in Fig. 2. As can be seen, the operation of basic subsystems was fully automated and monitored from the onset. As for the delicate closing of the detector halves, the operation first saw a commissioning phase, controlled by experts, and then became fully automated. A similar procedure was devised for the data quality monitoring. During the ongoing (first) long shutdown of the LHC, denoted LS1 in Fig. 2, a constant monitoring of the basic subsystems is carried out. For the second run of the LHC due by Spring 2015, no major changes on the operational aspects of the VELO are foreseen; only the monitoring of the data will become automated, following from ongoing developments building on the experience gained during Run I.

The VELO ran stably during Run I, with occasional issues being solved quickly by the on-call experts. For example, the temperature stability of the cooling system was roughly 0.1°C . And the yearly maintenance of the CO_2 pumps did not raise concerns; details of the operation of the cooling system are given in Ref. [3]. It should be noted that the operation of the VELO reached early on an efficiency of close to optimal, with the closing procedure taking a typical 210 seconds to complete.

The ST has also performed very well during the first three years of operation. Occasional problems were nevertheless encountered. On a regular basis, Vertical-Cavity Surface-Emitting Laser (VCSEL) diodes, which are used to transmit the optical data after off-detector digitisation,

died. The high failure rate of these oxide-confined VCSELs is recognised, and traced to manufacturing defects and mechanical stress creating cracks. On average one VCSEL was replaced per month.

In TT, various bond wires between the pitch adapter and the innermost bond row broke. Upon inspection, it was realised that the loop heights on the innermost rows were not high enough, which caused some mechanical stress, resulting in the observed breaks at the foot of the bonds. A certain number of hybrids was consequently produced with the “bond distance” increased, and the broken modules were removed and repaired. Increasing the distance between allowed to slightly increase the bond height for the inner rows without needing to increase the bond heights too much for the outer rows, which would then cause the outer rows to be weakened.

With beam in the machine, occasional large spikes in the HV system of TT produced trips. The reason was not fully understood, though cured by the installation of Kapton shielding.

5. Detector performance

5.1 Channel efficiencies

By the end of Run I the percentage of working channels for the VELO, TT and IT was calculated to be 99.27%, 99.61% and 98.41%, respectively, for a total number of detector channels of order 150k in all three cases. In the case of the ST the high efficiency required the replacement of many VCSEL diodes. The lower channel efficiency observed for IT stems from the difficult access for repairs; three diodes were in fact lost and not replaced.

5.2 Signal and noise

All tracking subdetectors show an excellent signal-over-noise (S/N) ratio and a low noise level. The S/N ratio for VELO, TT and IT lies between 12 and 21, being lowest for the high-capacitance TT strips and highest for the VELO Φ strips. All values are found to be within 10 – 20% of expectations.

5.3 Hit resolutions

The sensor hit resolution depends upon the strip pitch and the charge sharing between the clustered strips: the finer the strip pitch the more likely it is for deposited charge to be shared between several strips; and tracks intersecting the sensors at large angles relative to the normal to the sensor plane (the so-called projected angle) tend to spread more charge across adjacent strips.

The VELO hit resolution is considerably better than the binary resolution for all strip pitches and projected angles. The best resolution achieved, $4\mu\text{m}$, is obtained for the optimally angled tracks in the smallest pitch region.

The average hit resolutions for TT and IT are determined in a two-step procedure: first, the distribution of unbiased residuals for all clusters on tracks is obtained with a Kalman fit to tracks traversing the VELO and the ST stations. For each hit, the unbiased residual is calculated as the distance between the hit and the extrapolated position obtained from a track fit excluding that particular hit. Second, the biased sensor residual is defined as the mean of the unbiased residuals on the sensor. The RMS of the distribution of the biased residuals from all sensors is representative

of the alignment precision. The hit resolution is determined subtracting (in quadrature) the biased residual RMS from the RMS of the distribution of unbiased residuals. The average hit resolution for TT (IT) amounts to 59 (50) μm .

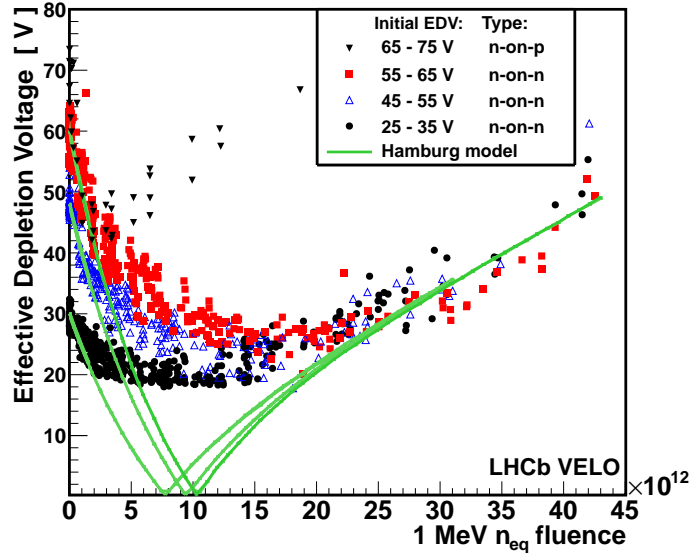


Figure 3: Effective depletion voltage versus fluence for the VELO during the period 2010-11. The data is compared to the predictions from the Hamburg model [4]. Refer to the text for details.

5.3.1 Radiation damage

Irradiation causes surface and bulk damage in the silicon. With high fluences up to $14 \times 10^{13} 1\text{MeV}n_{\text{eq}}/\text{cm}^2$ caused by the proximity of the proton beams, radiation damage has been monitored with particular care by the VELO group. Four independent and complementary methods of investigating radiation damage are considered: (1-2) dependence of sensor currents on voltage and temperature; (3) changes in depletion voltage; and (4) charge collection and cluster finding efficiencies. A full account of all methods implemented and studies performed for the VELO is given in Ref. [5]. Highlights are discussed hereafter for the three detectors.

The changes in depletion voltage are quantified studying the evolution of the so-called effective depletion voltage (EDV) as a function of the fluence the sensors receive. The method is as follows: all sensors are kept at the nominal voltage of 150 V except the test sensor, whose bias voltage is varied between 0 and 150 V. A track trajectory reconstructed leaving out the test sensor every fifth module is extrapolated to the latter, and the amount of charge collected computed. Thence a Landau distribution of the ADC counts is obtained at each voltage. The most probable value (MPV) of each Landau follows a raising curve that attains a plateau with high enough a bias voltage. The EDV is defined as the voltage at which the curve reaches 80% of the MPV plateau value.

¹Radiation damage is typically expressed as a multiple of the expected damage of a 1 MeV neutron, the so-called 1 MeV neutron equivalent, $1\text{MeV}n_{\text{eq}}/\text{cm}^2$.

The dependence of the EDV versus fluence for the period 2010-11 (corresponding to a total recorded luminosity of 1.1 fb^{-1}) is presented in Fig. 3. The EDV is seen to decrease with fluence² down to approximately 18 V until type inversion occurs around a fluence of $1.5 \times 10^{13} \text{ MeV} n_{\text{eq}}/\text{cm}^2$. The rise is then linear, as predicted by the Hamburg model [4], and found to be independent of the initial sensor EDV.

With an inner radius of 7 mm and an outer radius of 42 mm the VELO receives a large and non-uniform radiation dose. In this extreme and highly non-uniform radiation environment, type-inversion of the inner part of the n-on-n sensors has been measured. The situation is somewhat different for the n-on-p sensors: the initial EDV is found to decrease up to a fluence of approximately $2 \times 10^{12} \text{ MeV} n_{\text{eq}}/\text{cm}^2$, and then to increase with further fluence. Detailed studies are presented in Ref. [5].

The data is in general good agreement with the Hamburg model at low and high fluences, *i.e.* away from the type inversion region where the model is known to be inappropriate. Equivalent studies for the ST are ongoing.

The time evolution of the leakage current in both ST trackers is source of constant monitoring; Fig. 4 shows the peak current versus time for TT, where the peak current is defined as the maximum current during a fill of the LHC. The observed trend is in very good agreement with the amount of delivered integrated luminosity, which is superposed on the figure. The decrease of the peak current due to annealing in the silicon corresponds to periods of time with no colliding beams. Furthermore, the predictions are in excellent agreement with the observed evolution of the peak currents.

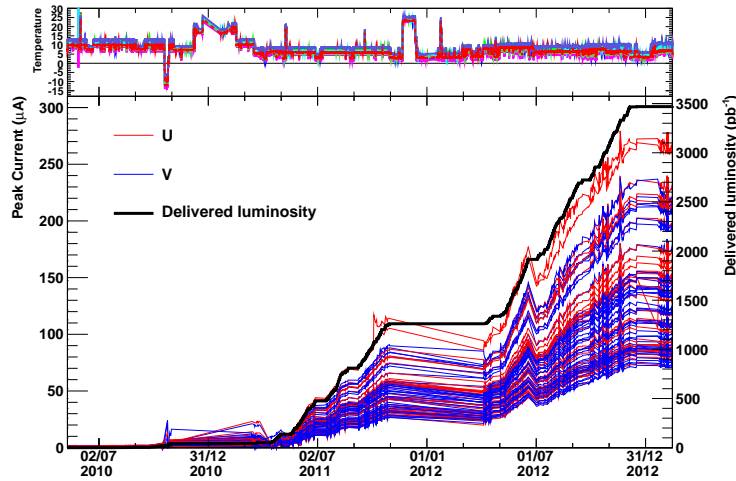


Figure 4: Measured peak current in TT versus time for the U and V stereo layers with tilts of -5° and $+5^\circ$, respectively. The delivered integrated luminosity is superposed. The temperature of the TT boxes is displayed for reference at the top of the figure.

²In practice, the EDV does not drop to zero since a minimal electric field in the sensor is required to collect the charge.

6. Physics performance

6.1 Alignment

As mentioned above, the VELO halves are closed and centered around the beam for each fill, once the LHC declares the beams stable. As a consequence, the beam position is determined on a fill-by-fill basis from a reconstruction of the primary interaction vertex using either tracks in the right or in the left half. The precision to which the two VELO halves are positioned around the beam-line, after closing, is determined from the distance between the two independently reconstructed vertices. For Run I the alignment of the VELO halves was found to be stable and within $5\ \mu\text{m}$.

The alignment studies for the ST rely on a global χ^2 minimisation based on Kalman track fit residuals [6]; improvements are obtained applying a mass constraint to vertices from $D^0 \rightarrow K^- \pi^+$ decays [7]. The alignment precision of the ST is determined to be approximately $14\ \mu\text{m}$.

6.2 Cluster finding efficiencies

The cluster finding efficiency (CFE) for a given (test) sensor of the VELO is determined by excluding the test sensor in pattern recognition and interpolating tracks to it. To avoid biases due for example to fake tracks, quality cuts are applied to the samples. Furthermore, tracks are required to have hits in at least six modules, with hits on both R and Φ sensors of the two sensors in front of and behind the test sensor. Considering all detector channels, a CFE of $(99.51 \pm 0.02)\%$ is found for the VELO. The CFE increases to $(99.98 \pm 0.02)\%$ once known defective strips are excluded.

6.3 Primary vertex resolutions

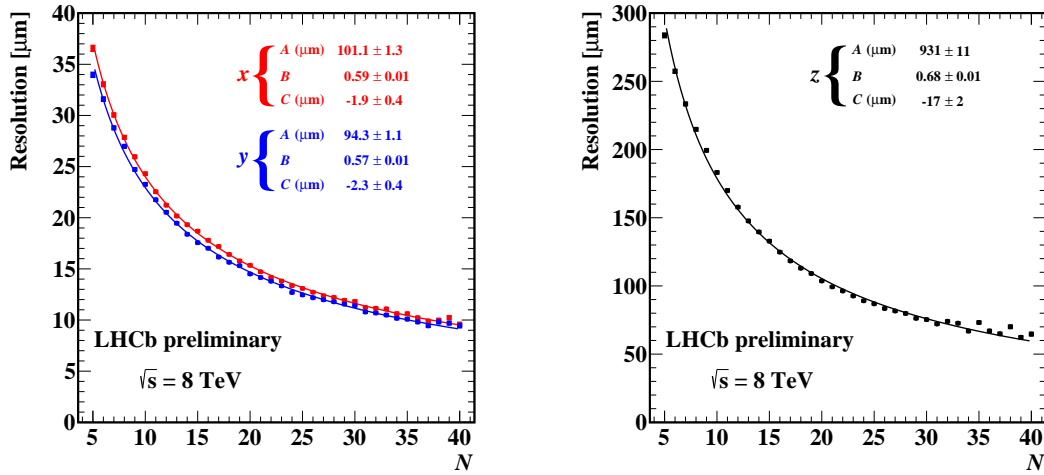
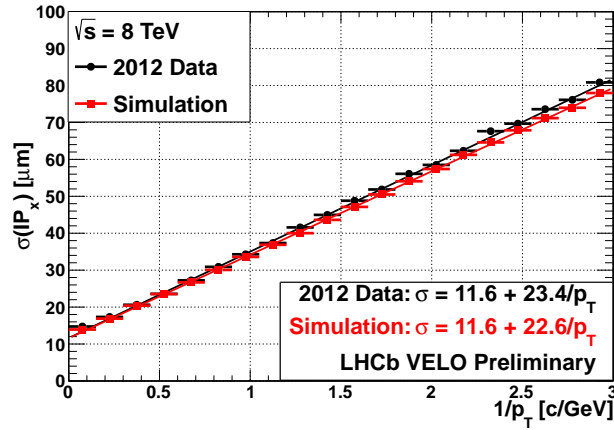
Primary vertices at LHCb are fitted using an adaptive method that minimises the average χ_{IP}^2 of the tracks used in the fit [8]. The PV resolution is evaluated by splitting the tracks used to fit a PV into two sets, and fitting a PV with each set, then examining the distance between the two resulting PVs. The resolutions on the coordinates transverse to the beam-line determined using 2012 data and simulation are shown in Fig. 5 as a function of the number of tracks (N) used to fit the PV. All data points are fitted with an empirical function of the form $(A/N^B) + C$, A , B and C being the fitted model parameters.

For a one-PV event with a typical number of tracks $N = 25$, the resolutions in the transverse plane and along the beam-line are $\sigma_{x,y} \sim 13\ \mu\text{m}$ and $\sigma_z \sim 90\ \mu\text{m}$, respectively. These values increase slightly with increasing pile-up, *i.e.* with an increasing number of reconstructed PVs. For a matter of comparison, the resolution along the beam-line increases to $\sigma_z \sim 100\ \mu\text{m}$ (again for a PV with 25 tracks) for a three-PV event.

6.4 Impact parameter resolutions

The typical signature of daughter particles from a heavy hadron decay is their large impact parameter (IP), where the IP of a track is defined as the distance of closest approach to a PV. Most analyses at LHCb rely on IP – among other selection criteria – to disentangle (short lived) background from heavy flavoured hadron decays.

The IP resolution depends on the hit resolution; the detector material budget a track traverses, which determines the amount of multiple scattering; and the extrapolation distance between the

Figure 5: Primary vertex resolutions (left) in x and y and (right) in z .Figure 6: IP resolution (x component) as a function of the inverse track transverse momentum p_T . The result obtained from simulation is superposed to the data.

interaction point and the sensitive region of the detector. It is well modelled empirically with a linear dependence on the inverse of the transverse momentum (p_T) of the track, as observed in Fig. 6. For high- p_T tracks an excellent IP resolution around $12\mu\text{m}$ is achieved. Figure 6 also displays a comparison with simulation; there is good agreement. In particular, the slope of the p_T dependence is in excellent agreement, which reflects an accurate description of the detector material in simulation. Details are to be found in Ref. [9].

Parameter	VELO	TT	IT
Signal-over-noise ratio	19 – 21	12 – 15	≈ 17
Single-hit resolutions	4-25 μm	59 μm	50 μm
Cluster finding efficiencies	99.5%	99.3%	99.7%
Tracking efficiency for Long tracks	$\approx 98\%$		
Typical PV resolutions (25 tracks/vertex)	13 (90) in $x, y (z)$		
Typical IP resolutions	$\approx 12 \mu\text{m}$ in x, y (2012 data)		

Table 1: Summary of the performance of the silicon trackers.

7. Outlook

In conclusion, the silicon trackers of LHCb have performed very well and smoothly over the whole period of the first run of the LHC. A summary of the main parameters describing the excellent performance is given in Table 1.

Radiation damage effects have been studied with various complementary methods, and are continuously monitored. Type inversion has been observed in the VELO, but not in either of the ST detectors. Radiation damage has so far no impact on the quality of the physics results.

References

- [1] LHCb collaboration, A. A. Alves Jr. *et al.*, *The LHCb detector at the LHC*, *JINST* **3** (2008) S08005.
- [2] D. van Eijk *et al.*, *Radiation hardness of the LHCb Outer Tracker*, *Nucl. Instrum. Meth.* **A685** (2012) 62.
- [3] E. Jans. These proceedings.
- [4] R. Wunstorf *et al.*, *Results on radiation hardness of silicon detectors up to neutron fluences of $10^{15}n/\text{cm}^2$* , *Nucl. Instrum. Meth.* **A315** (1992) 149.
- [5] A. Affolder *et al.*, *Radiation damage in the LHCb vertex locator*, *JINST* **8** (2013) P08002, [arXiv:1302.5259](https://arxiv.org/abs/1302.5259).
- [6] W. Hulsbergen, *The global covariance matrix of tracks fitted with a kalman filter and an application in detector alignment*, *Nucl. Instrum. Meth.* **A600** (2009) 471 .
- [7] J. Amoraal *et al.*, *Application of vertex and mass constraints in track-based alignment*, *Nucl. Instrum. Meth.* **A712** (2013) 48 .
- [8] M. Krasowski *et al.*, *Primary vertex reconstruction*, [LHCb-2007-011](#).
- [9] A. Affolder *et al.*, *Performance of the LHCb vertex locator*, to be submitted to JINST.